Chinese Journal of Catalysis 35 (2014) 1385–1393 催化学报 2014年 第35卷 第8期 | www.chxb.cn

available at www.sciencedirect.com

ScienceDirect

journal homepage: www.elsevier.com/locate/chnjc

Article (Special Issue on Rare Earth Catalysis)

^{18}O isotopic study of photo-induced formation of peroxide species on cubic Nd_2O_3

Xiaolian Jing, Wenyu She, Weizheng Weng *, Jianmei Li, Wensheng Xia, Huilin Wan #

State Key Laboratory of Physical Chemistry of Solid Surfaces, National Engineering Laboratory for Green Chemical Productions of Alcohols, Ethers and Esters and Department of Chemistry, College of Chemistry and Chemical Engineering, Xiamen University, Xiamen 361005, Fujian, China

ARTICLE INFO

Article history:
Received 28 March 2014
Accepted 14 May 2014
Published 20 August 2014

Keywords:
Oxygen activation
Peroxide
Neodymium sesquioxide
Photo-induced reaction
^{18}O isotopic study
Raman spectroscopy

ABSTRACT

Photo-induced formation of peroxide species on cubic Nd_2O_3 was studied by *in situ* microprobe Raman spectroscopy using ^{18}O as a tracer and a 325-nm laser as an excitation source. The results confirmed that the peroxide ions were formed through photooxidation of the lattice oxygen species in neodymium sesquioxide by molecular oxygen species. Under UV excitation (λ = 325 nm), the reaction between O_2 and O^{2-} could take place at room temperature. A fast oxygen exchange between the peroxide ions and the lattice oxygen species in Nd_2O_3 took place under the experimental conditions studied. Also, bulk lattice oxygen species in Nd_2O_3 could migrate to the surface layer and participate in the formation of peroxide ions. The migration of lattice oxygen species and the oxygen exchange between lattice oxygen and peroxide ions were promoted by UV laser irradiation.

1. Introduction

Owing to their excellent electronic characteristics and chemical and thermal stabilities, lanthanide oxides have been widely used as catalysts in the catalytic oxidation of light alkanes such as oxidative coupling of methane and oxidative dehydrogenation of ethane [1–12]. Understanding the role of activated forms of oxygen species and pathways of O_2 activation on the lanthanide oxides is therefore of fundamental importance to the above-mentioned reactions [13–19]. Our study of Ln_2O_3 (Ln = La, Nd, Sm, Gd) under O_2 by microprobe laser Raman spectroscopy revealed that laser excitation could induce the formation of peroxide species on the Ln_2O_3 surface [20,21]. Thus, a new pathway towards molecular oxygen activation under mild conditions was discovered that presents potential application in photocatalytic reactions. Additionally, the study provided new insights in the mechanism of O_2 activation on the surface of metal oxides with stable cationic valence. In continuation of the previous research, here we examine the formation of peroxide on cubic Nd_2O_3 using ^{18}O as tracer, aiming at further understanding the mechanisms of the photo-induced formation of peroxide ions on lanthanide sesquioxides with stable cationic valence.

2. Experimental

2.1. Sample preparation

Cubic Nd_2O_3 was prepared from $Nd(OH)_3$ according to reported procedures [22,23]. First, commercial Nd_2O_3 (99.99%,

* Corresponding author. Tel/Fax: +86-592-2185192; E-mail: wzweng@xmu.edu.cn
# Corresponding author. Tel: +86-592-2186569; Fax: +86-592-2185192; E-mail: hlwan@xmu.edu.cn

This work was supported by the National Basic Research Program of China (973 Program, 2010CB732303), the National Natural Science Foundation of China (21173173, 21033006, 21373169), and the Program for Changjiang Scholars and Innovative Research Team in University (IRT1036).
DOI: 10.1016/S1872-2067(14)60153-4 | http://www.sciencedirect.com/science/journal/18722067 | Chin. J. Catal., Vol. 35, No. 8, August 2014

Alfa Aesar) was treated at 100 °C for 100 h with a 21% O_2/N_2 flow containing water vapor (by bubbling 21% O_2/N_2 through H_2O at room temperature) to form $Nd(OH)_3$. Then, $Nd(OH)_3$ was heated at 650 °C in a flow of 21% O_2/N_2 (50 mL/min) for 3 h to produce Nd_2O_3.

2.2. Sample characterization

The crystalline structure of the sample was confirmed by X-ray powder diffraction (XRD) analysis to be cubic Nd_2O_3 (Fig. 1). The experiment was carried out on a PANalytical X'pert PRO diffractometer using Cu K_α radiation, operating at 40 kV and 30 mA. The Brunauer-Emmett-Teller (BET) surface area of Nd_2O_3 is 6.9 m^2/g as measured by N_2 adsorption-desorption analysis at −196 °C on a Micromeritics TriStar II 3020. Before the measurement, the sample was degassed at 200 °C for 3 h. The scanning electron microscopy (SEM) image of the sample (Fig. 2) was obtained on a Hitachi S-4800 scanning electron microscope operating at an accelerating voltage of 15 kV. Sample preparation consists of depositing a drop of Nd_2O_3/ethanol suspension on a clean silicon substrate.

2.3. Raman spectroscopy characterization

Raman spectra were recorded on a Renishaw R1000 microprobe Raman spectrometer equipped with a charge-coupled device (CCD) detector using a 325-nm He-Cd laser as the excitation source and an in-house-built high-temperature *in situ* Raman cell specifically designed for the spectrometer. A diagram of the Raman cell is available elsewhere [24]. The microscope attachment for the spectrometer was based on a Leica DMLM system equipped with an OFR LMU-15×-NUV objective. The spectra acquisition time was varied according to the different experiments; an acquisition time of 50 s was typically used. The laser spot on the sample was about 3 μm in diameter, and the spectral resolution was ~6 cm^{-1}. The maximum laser power of the spectrometer measured at the analysis spots was about 3 mW. However, a laser power of 0.75 mW was used in most experiments.

For the experiments performed on cubic $Nd_2{}^{16}O_3$, the sample was first heated under flowing $^{16}O_2$ (50 mL/min, 99.995%, Linde) at 650 °C for 180–360 min to remove carbonate species and moisture. The treated $Nd_2{}^{16}O_3$ was then cooled in the dark

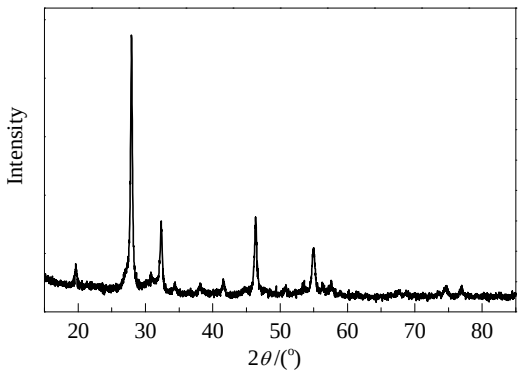

Fig. 1. XRD pattern of the prepared cubic Nd_2O_3.

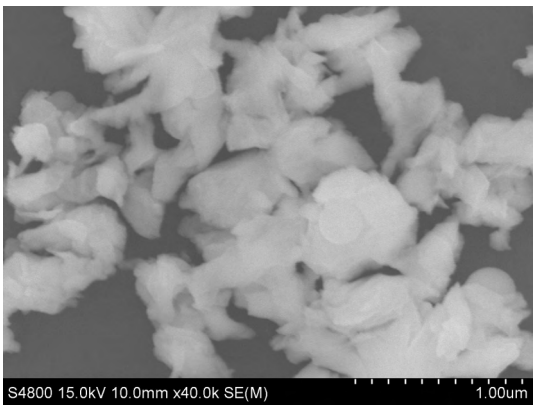

Fig. 2. SEM image of the prepared cubic Nd_2O_3.

to 25 °C under $^{16}O_2$ before it was exposed to a focused 325-nm laser beam from the Raman spectrometer to induce formation of peroxide ions, and the resulting spectra were recorded under either $^{18}O_2$ or $^{16}O_2$ atmosphere.

The ^{18}O-labeled Nd_2O_3 was obtained by treating cubic $Nd_2{}^{16}O_3$ with a flow of $^{18}O_2$ (5 mL/min, 97%, CIL) at 650 °C for 6 h. The sample was then cooled in the dark under $^{18}O_2$ to 25 °C. The treated sample (^{18}O-labeled Nd_2O_3) was then exposed to a focused 325-nm laser beam to induce formation of peroxide ions, and the resulting spectra were recorded under $^{18}O_2$ atmosphere.

3. Results and discussion

3.1. Photo-induced formation of peroxide species on $Nd_2{}^{16}O_3$ under $^{16}O_2$ and $^{18}O_2$ atmospheres

Fig. 3(a) shows the changes in the Raman spectra when cubic $Nd_2{}^{16}O_3$ was irradiated at varying times under $^{16}O_2$ atmosphere with a focused 325-nm laser beam at 25 °C. As observed, the Raman band at 833 cm^{-1}, which represents the O–O stretching mode ($\nu_{O\text{-}O}$) of the $^{16}O_2{}^{2-}$ peroxide species [20,21, 25–27], began to grow at the expense of the Nd^{3+}–$^{16}O^{2-}$ band at 331 cm^{-1}. Following irradiation with the laser at 25 °C for more than 60 min, the Raman spectrum of the sample was recorded in the frequency range of 1300–1800 cm^{-1} and shown in Fig. 3(b). Two bands at 1554 and 1646 cm^{-1} could be clearly identified. The broad band at 1646 cm^{-1} could be assigned to the overtone of the O–O stretching vibration of the $^{16}O_2{}^{2-}$ peroxide species because its wavenumber was almost twice that of the band at 833 cm^{-1}. The narrow band at 1554 cm^{-1} could be assigned to molecular oxygen species; the O–O stretching vibration of the gas phase $^{16}O_2$ molecule could be observed at a comparable wavenumber (Fig. 4). Considering that the wavenumber of the molecular oxygen band in Fig. 3(b) shifts by ~2 cm^{-1} towards lower frequencies when compared with that of the gas phase $^{16}O_2$, the band at 1554 cm^{-1} can be attributed to a $^{16}O_2$ species adsorbed on the surface of Nd_2O_3. This band may be due to the decomposition of the peroxide species. Further evidence of the origin of the 1554 cm^{-1} Raman band is presented in Section 3.2.

Fig. 5(a) shows the changes in the Raman spectra of cubic

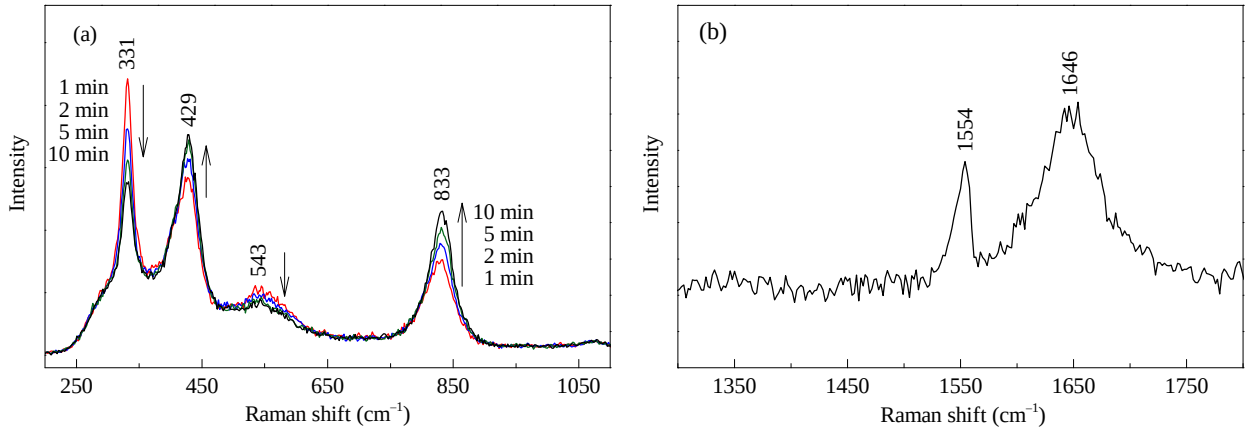

Fig. 3. (a) *In situ* Raman spectra of cubic $Nd_2{}^{16}O_3$ irradiated at varying times with a focused 325-nm laser beam under $^{16}O_2$ at 25 °C. (b) Raman spectrum (frequency range of 1300–1800 cm^{-1}) of cubic $Nd_2{}^{16}O_3$ following irradiation with a 325-nm laser under $^{16}O_2$ at 25 °C for more than 60 min. The laser power used to induce formation of the peroxide species was 0.75 mW.

$Nd_2{}^{16}O_3$ under $^{18}O_2$ upon continuous irradiation with a focused 325-nm laser beam at 25 °C. The spectra are very similar to those shown in Fig. 3(a). The onset of a peroxide Raman band corresponding to $^{16}O_2{}^{2-}$ was observed at the expense of the Nd^{3+}–$^{16}O^{2-}$ stretching band at 335 cm^{-1}. This observation clearly indicates that lattice oxygen ($^{16}O^{2-}$) species in Nd_2O_3 are involved in the formation of peroxide ions. Fig. 5(b) shows the Raman spectrum in the frequency range of 1300–1800 cm^{-1} of the $Nd_2{}^{16}O_3$ sample following irradiation with a 325-nm laser beam at 25 °C under $^{18}O_2$ for more than 30 min. In addition to the O–O stretching vibration of the $^{16}O_2$ molecule at 1554 cm^{-1} and the overtone of the O–O stretching vibration of the $^{16}O_2{}^{2-}$ peroxide ions at ~1640 cm^{-1}, a new band at 1471 cm^{-1} corresponding to the O–O stretching vibration of gas phase $^{18}O_2$ (Fig. 4) was observed. Considering that $^{18}O_2$ is the major component (isotope purity >97%) in the gas phase, and that the Raman peak intensity of $^{16}O_2$ in Fig. 5(b) is much higher than that of the gas phase $^{18}O_2$, the peak at 1554 cm^{-1} can be rationally assigned to surface $^{16}O_2$ species. Because the 1554 cm^{-1} band could only be detected after the formation of peroxide species, its appearance was attributed to the decomposition of the $^{16}O_2{}^{2-}$ peroxide ions, probably through a photo-decomposition reaction induced by irradiation with the 325-nm laser. Decomposition of $Nd_2O_2(O_2)$ was reportedly observed following long exposure with a 488-nm Ar^+ laser [28].

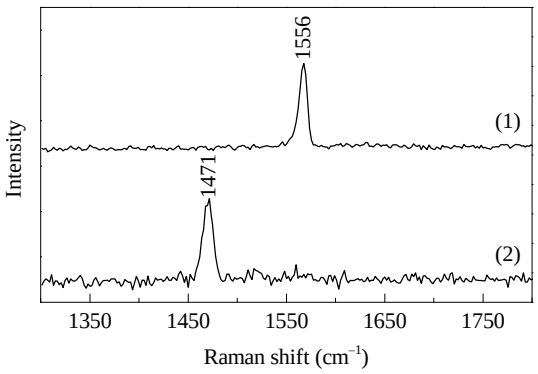

Fig. 4. Raman spectra of gas phase $^{16}O_2$ (1) and $^{18}O_2$ (2) recorded with a 325-nm laser at 25 °C.

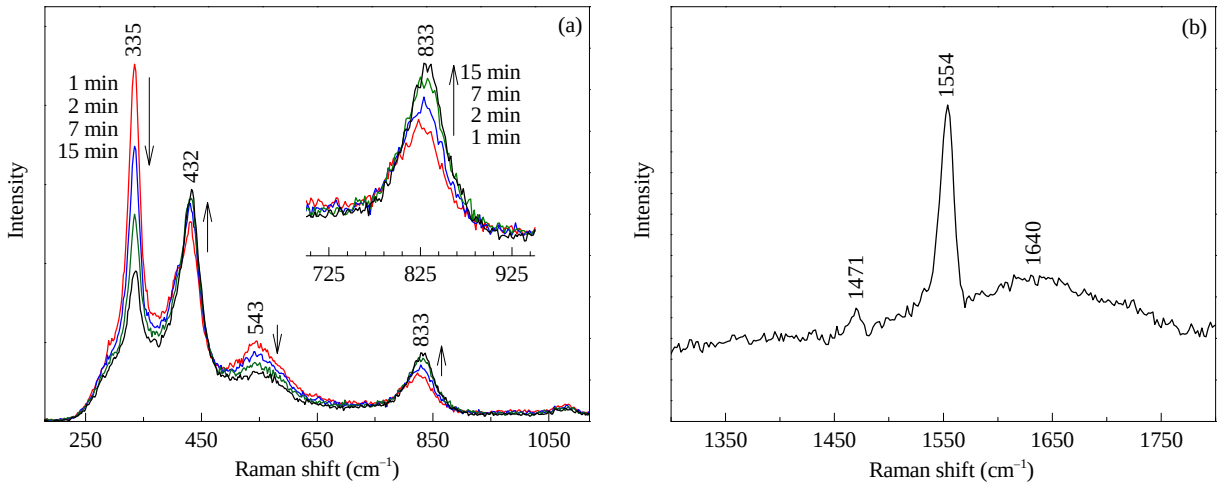

Fig. 5. (a) *In situ* Raman spectra of cubic $Nd_2{}^{16}O_3$ irradiated at varying times with a focused 325-nm laser beam under $^{18}O_2$ at 25 °C. (b) Raman spectrum (frequency range of 1300–1800 cm^{-1}) of cubic $Nd_2{}^{16}O_3$ following irradiation with a 325-nm laser under $^{18}O_2$ at 25 °C for more than 30 min. The laser power used to induce formation of the peroxide species was 0.75 mW.

As suggested in the previous studies [20,21], the peroxide ions on lanthanide sesquioxides are generated by a photo-induced oxidation of lattice oxygen species by molecular oxygen because molecular oxygen species are always required in the formation of peroxide ions. Thus, for a reaction using $^{18}O_2$ and $^{16}O^{2-}$ as reactants, the peroxide ions should be labeled with ^{18}O atoms. However, in the Raman spectra shown in Fig. 5(a), only the peroxide ions containing ^{16}O atoms were detected. This phenomenon may have resulted from a fast oxygen isotope exchange between lattice oxygen and the peroxide species under the experimental conditions studied. Because $^{16}O^{2-}$ ions are the most abundant isotope oxygen species on the Nd_2O_3 surface, a fast isotope exchange between $^{16}O^{2-}$ and ^{18}O-labeled peroxide ions will lead to the formation of $^{16}O_2^{2-}$ on the Nd_2O_3 surface. Owing to the fast isotope exchange between lattice oxygen and surface dioxygen (peroxide and molecular oxygen) species, the isotope oxygen atoms in the peroxide ions (833 cm^{-1}) were identical to the isotope oxygen atoms in the surface molecular oxygen species (1554 cm^{-1}), resulting from the decomposition of the peroxide ions. This is also evidenced by the absence of Raman bands corresponding to molecular oxygen species with mixed isotope oxygen atoms ($^{18}O^{16}O$) (Fig. 5(b)). These results suggest that the Raman signals of the isotope-labeled surface molecular oxygen species can be used to identify the isotope-labeled peroxide ions formed on the surface of Nd_2O_3 using ^{18}O as a tracer. The advantage of using Raman peaks corresponding to surface molecular oxygen species towards the identification of isotope-labeled peroxide ions is that the Raman peaks associated with surface molecular oxygen species are significantly narrower than that associated with peroxide ions. Hence, a better resolution can be achieved.

3.2. *Photo-induced formation of peroxide species on ^{18}O-labeled Nd_2O_3 under $^{18}O_2$*

To gain further insights into the mechanisms of the photo-induced formation of peroxide ions on Nd_2O_3, the experiments were performed with cubic Nd_2O_3 partially labeled with ^{18}O. The sample was prepared by treating cubic $Nd_2{}^{16}O_3$ with a flow of $^{18}O_2$ at 650 °C for 6 h followed by cooling under $^{18}O_2$ to 25 °C. After the treatment, the characteristic metal–oxygen vibration band of neodymium sesquioxide shifted from 336 to 320 cm^{-1}. The position of the latter band is comparable with the band position of Nd^{3+}–$^{18}O^{2-}$ (319 cm^{-1}), as calculated based on the wavenumber of Nd^{3+}–$^{16}O^{2-}$ at 336 cm^{-1} by assuming a simple harmonic oscillator model. This result also indicates that almost all of the $^{16}O^{2-}$ atoms on the surface of Nd_2O_3 microcrystal (at least those within the detection depth of the Raman spectrometer) are replaced by $^{18}O^{2-}$. Fig. 6(a) shows the changes in the Raman spectra of an ^{18}O-labeled Nd_2O_3 sample upon irradiation at varying times with a focused 325-nm laser beam under $^{18}O_2$ at 25 °C. The spectrum recorded after 1 min irradiation revealed a band with maximum at 789 cm^{-1}. With increasing photo irradiation time, a shoulder band at 811 cm^{-1} appeared. This band became noticeable after the sample was irradiated for 15 min. Following irradiation of the ^{18}O-labeled Nd_2O_3 sample under $^{18}O_2$ with a 325-nm laser for more than 30 min, the Raman spectrum of the sample was recorded in the frequency range of 1300–1800 cm^{-1}, and the result is shown in Fig. 6(b). Three sharp peaks at 1468, 1510, and 1554 cm^{-1} were observed. A simple calculation based on the diatomic harmonic oscillator model using the $\nu_{O\text{-}O}$ band of a $^{16}O_2^{2-}$ peroxide ion at 833 cm^{-1} gave band positions at 786 and 810 cm^{-1} for the $^{18}O_2^{2-}$ and $(^{18}O^{16}O)^{2-}$ peroxide ions, respectively. Similarly, the calculation using the $\nu_{O\text{-}O}$ band of a $^{16}O_2$ molecule at 1556 cm^{-1} gave band positions at 1467 and 1512 cm^{-1} for $^{18}O_2$ and $^{18}O^{16}O$, respectively. As observed, the calculated band positions for the ^{18}O-labeled peroxide ions and molecular oxygen species are in good agreement with the experimental results shown in Fig. 6. Because the experiment was performed under flowing $^{18}O_2$ with isotope purity higher than 97%, the 1510 and 1554 cm^{-1} peaks observed in Fig. 6(b) can be solely attributed to molecular oxygen species ($^{18}O^{16}O$ and $^{16}O_2$) on the surface of the ^{18}O-labeled Nd_2O_3 sample. Considering that the intensity ratio

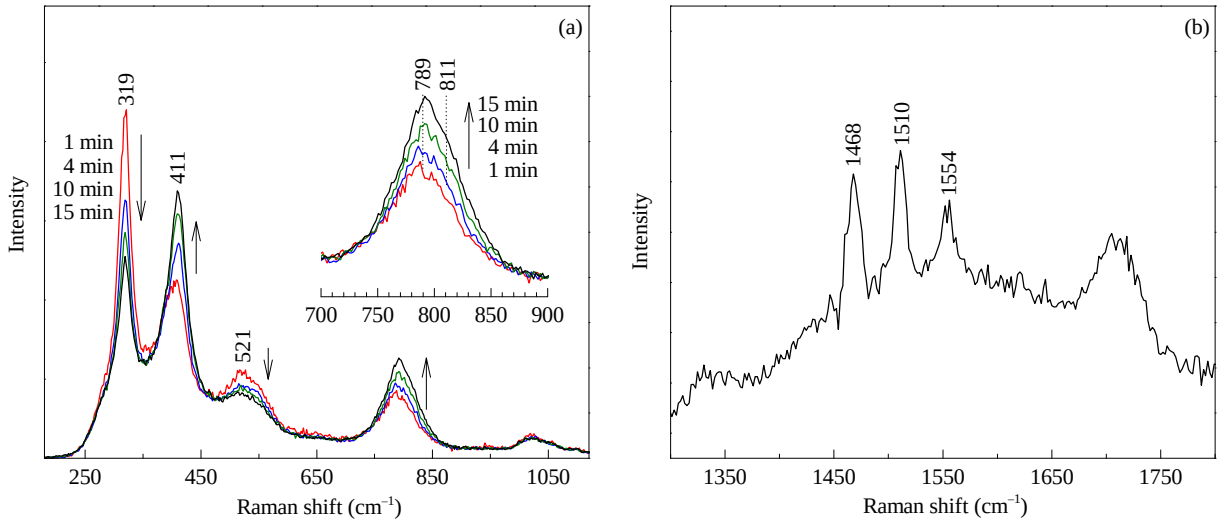

Fig. 6. (a) *In situ* Raman spectra of ^{18}O-labeled cubic Nd_2O_3 irradiated at varying times with a focused 325-nm laser beam under $^{18}O_2$ at 25 °C. (b) Raman spectrum (frequency range of 1300–1800 cm^{-1}) of the ^{18}O-labeled cubic Nd_2O_3 sample following irradiation with a 325-nm laser under $^{18}O_2$ at 25 °C for more than 30 min. The laser power used to induce formation of the peroxide species was 0.75 mW.

of the $^{18}O_2$ and $^{16}O_2$ peaks in Fig. 6(b) is much higher than that in Fig. 5(b), and that the wavenumber of the $^{18}O_2$ peak in Fig. 6(b) shifts by ~3 cm^{-1} towards lower frequencies when compared with that of the gas phase $^{18}O_2$ (Fig. 4), the peak at 1468 cm^{-1} can also be rationally assigned to surface $^{18}O_2$ species. Based on the results and the analysis given in Section 3.1, it can be concluded that three isotope-labeled peroxide ions (i.e., $^{18}O_2^{2-}$, $(^{18}O^{16}O)^{2-}$, and $^{16}O_2^{2-}$) are formed under the experimental conditions studied. Because the experiment was performed under $^{18}O_2$ atmosphere, the ^{16}O atoms detected in the peroxide ions and molecular oxygen species can only originate from the ^{18}O-labeled Nd_2O_3 prepared by treating $Nd_2{}^{16}O_3$ with $^{18}O_2$. The observed Raman bands corresponding to ^{16}O-labeled peroxide ions (at 811 cm^{-1}) and surface molecular oxygen species (at 1510 and 1554 cm^{-1}) provided further evidence of the involvement of lattice oxygen species in the formation of peroxide ions. These results also indicated that even though the $Nd_2{}^{16}O_3$ sample was treated with $^{18}O_2$ at 650 °C for 6 h, lattice oxygen species in the bulk phase of Nd_2O_3 microcrystals were not fully replaced by $^{18}O^{2-}$.

Based on the changes in the Raman spectra shown in Fig. 6, it can be deduced that molecular $^{18}O_2$ first reacts with the $^{18}O^{2-}$ species on the surface of the ^{18}O-labeled Nd_2O_3 microcrystals because most of the surface lattice oxygen species have been replaced by $^{18}O^{2-}$, leading to the formation of $^{18}O_2^{2-}$ peroxide ions (789 cm^{-1}). With increasing laser irradiation time, the $^{16}O^{2-}$ species in the bulk phase also participated in the formation of peroxide ions, as evidenced by the presence of $(^{18}O^{16}O)^{2-}$ peroxide ion (811 cm^{-1}), and $^{18}O^{16}O$ (1510 cm^{-1}) and $^{16}O_2$ (1554 cm^{-1}) molecular oxygen species on the surface of the sample. The $(^{18}O^{16}O)^{2-}$ peroxide ions could have resulted from either the migration of the $^{16}O^{2-}$ species from the bulk phase of the ^{18}O-labeled Nd_2O_3 microcrystals to the surface layer followed by isotope exchange with the $^{18}O_2^{2-}$ peroxide ions or direct photo-induced reaction between $^{16}O^{2-}$ and $^{18}O_2$. The $(^{18}O^{16}O)^{2-}$ peroxide ions can then transform to $^{16}O_2^{2-}$ through isotopic exchange with $^{16}O^{2-}$. The migration of lattice $^{16}O^{2-}$ species from bulk to surface layer and the isotope exchange between $^{16}O^{2-}$ and $^{18}O_2^{2-}$ could be induced (or promoted) by the UV (λ = 325 nm) laser irradiation. To obtain experimental evidence, the effect of photo irradiation power on the formation of peroxide ions was studied. The experiments were performed by irradiating an ^{18}O-labeled cubic Nd_2O_3 sample under $^{18}O_2$ with laser powers of 0.3 and 3 mW at 25 °C. As shown in Fig. 7(a), the Raman spectra obtained with a laser power of 0.3 mW only revealed a peroxide band, corresponding to $^{18}O_2^{2-}$ (790 cm^{-1}), within 14 min of photo irradiation, indicating that only the lattice oxygen species from the surface layer of the sample ($^{18}O^{2-}$) participated in the reaction with $^{18}O_2$. This observation further indicates that migration of $^{16}O^{2-}$ from the bulk phase to the surface layer and the isotope exchange between $^{16}O^{2-}$ and $^{18}O_2^{2-}$ can be neglected under the experimental conditions studied. However, when the laser power was raised to 3 mW (Fig. 7(b)), the band width of the peroxide Raman peak increased, and both the Raman bands corresponding to $^{18}O_2^{2-}$ (790 cm^{-1}) and $(^{18}O^{16}O)^{2-}$ (811 cm^{-1}) peroxide ions could be identified after the sample was irradiated for 5–20 min. This result clearly indicates that UV laser irradiation has an impact on the migration of lattice oxygen species and the oxygen exchange between lattice oxygen and peroxide ions. The photo-induced isotopic exchange between $^{18}O_2$ and lattice oxygen on TiO_2 at room temperature was previously reported in the literature [29,30].

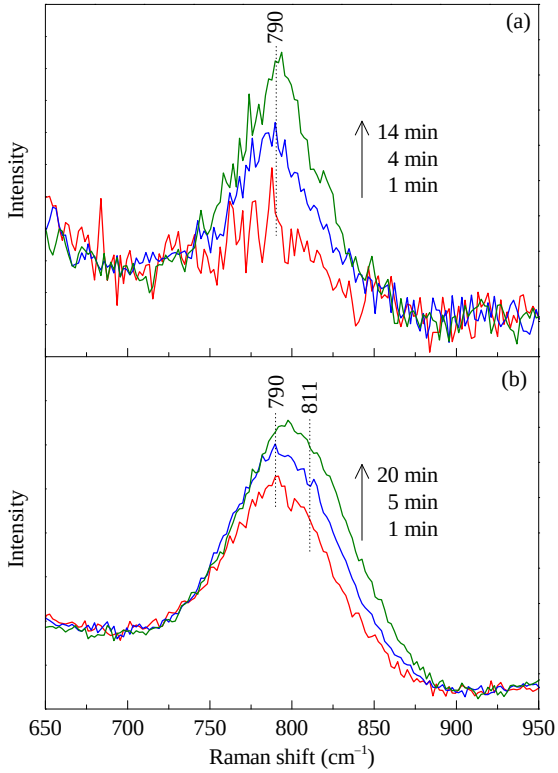

Fig. 7. Peroxide Raman bands formed upon irradiation of ^{18}O-labeled cubic Nd_2O_3 with a focused 325-nm laser beam, operating at a power of 0.3 (a) and 3 mW (b) under $^{18}O_2$ at 25 °C.

4. Conclusions

Molecular oxygen can be transformed to peroxide ions by a photo-induced reaction with lattice oxygen species of neodymium sesquioxide. Under UV excitation (λ = 325 nm), the reaction between O_2 and O^{2-} can take place at room temperature. The experimental studies involving ^{18}O as tracer indicated that fast oxygen exchange between peroxide ions and lattice oxygen species in Nd_2O_3 took place under the conditions studied, and that bulk lattice oxygen species in Nd_2O_3 could migrate to the surface layer and participate in the formation of peroxide species. The migration of lattice oxygen species and the oxygen exchange between lattice oxygen and peroxide ions were promoted by UV laser irradiation.

References

[1] Martin G A, Bernal S, Perrichon V, Mirodatos C. *Catal Today*, 1992, 13: 487
[2] Au C T, Chen K D, Ng C F. *Appl Catal A*, 1998, 170: 81
[3] Buyevskaya O V, Wolf D, Baerns M. *Catal Today*, 2000, 62: 91

Graphical Abstract

Chin. J. Catal., 2014, 35: 1385–1393 doi: 10.1016/S1872-2067(14)60153-4

^{18}O isotopic study of photo-induced formation of peroxide species on cubic-Nd_2O_3

Xiaolian Jing, Wenyu She, Weizheng Weng*, Jianmei Li, Wensheng Xia, Huilin Wan*
Xiamen University

Peroxide species can be generated through a photo-induced reaction between molecular oxygen and lattice oxygen of cubic neodymium sesquioxide. Both surface and bulk lattice oxygen species are involved in the formation of the peroxide species.

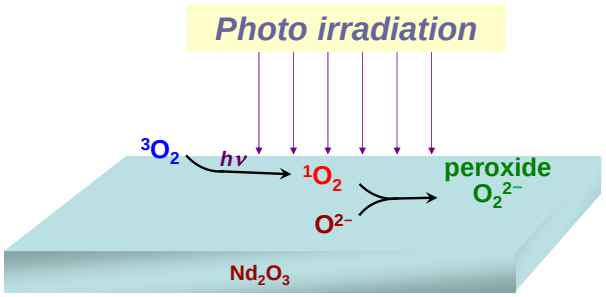

[4] Håkonsen S F, Holmen A. In: Ertl G, Knözinger H, Schüth F, Weitkamp J eds. Handbook of Heterogeneous Catalysis. New York: Wiley-VCH Verlag GmbH & Co KGaA, 2008. 3384
[5] Wan H L, Zhou X P, Weng W Z, Long R Q, Chao Z S, Zhang W D, Chen M S, Luo J Z, Zhou S Q. *Catal Today*, 1999, 51: 161
[6] Dedov A G, Loktev A S, Moiseev I I, Aboukais A, Lamonier J F, Filimonov I N. *Appl Catal* A, 2003, 245: 209
[7] Olivier L, Haag S, Pennemann H, Hofmann C, Mirodatos C, van Veen A C. *Catal Today*, 2008, 137: 80
[8] Lunsford J H. *Catal Today*, 1990, 6: 235
[9] Hou Y H, Chang G, Weng W Z, Xia W S, Wan H L. *Chin J Catal* (侯玉慧, 常刚, 翁维正, 夏文生, 万惠霖. 催化学报), 2011, 32: 1531
[10] Wang L H, Yi X D, Weng W Z, Wan H L. *Chin J Catal* (王丽华, 伊晓东, 翁维正, 万惠霖. 催化学报), 2006, 27: 653
[11] Hou Y H, Lin Y L, Li Q, Weng W Z, Xia W S, Wan H L. *ChemCatChem*, 2013, 5: 3725
[12] Ferreira V J, Tavares P, Figueiredo J L, Faria J L. *Catal Commun*, 2013, 42: 50
[13] Huang S J, Walters A B, Vannice M A. *J Catal*, 2000, 192: 29
[14] Lacombe S, Zanthoff H, Mirodatos C. *J Catal*, 1995, 155: 106
[15] Winter E R S. *J Chem Soc A*, 1969: 1832
[16] Palmer M S, Neurock M, Olken M M. *J Phys Chem B*, 2002, 106: 6543
[17] Mestl G, Knözinger H, Lunsford J H. *Ber Bunsen-Ges*, 1993, 97: 319
[18] Liu Y D, Zhang H B, Lin G D, Liao Y Y, Tsai K R. *J Chem Soc, Chem Commun*, 1994: 1871
[19] Xia W S, Zhang D, Weng W Z, Wan H L. *Chin J Catal* (夏文生, 张达, 翁维正, 万惠霖. 催化学报), 2013, 34: 2130
[20] Weng W Z, Wan H L, Li J M, Cao Z X. *Angew Chem Int Ed*, 2004, 43: 975
[21] Jing X L, Chen Q C, He C, Zhu X Q, Weng W Z, Xia W S, Wan H L. *Phys Chem Chem Phys*, 2012, 14: 6898
[22] Shafer M W, Roy R. *J Am Ceram Soc*, 1959, 42: 563
[23] Tong J, Eyring L. *J Alloys Compd*, 1995, 225: 139
[24] Weng W Z, Pei X Q, Li J M, Luo C R, Liu Y, Lin H Q, Huang C J, Wan H L. *Catal Today*, 2006, 117: 53
[25] Eysel H H, Thym S. *Z Anorg Allg Chem*, 1975, 411: 97
[26] Heyns A M, Range K J. *J Raman Spectrosc*, 1994, 25: 855
[27] Hesse W, Jansen M, Schnick W. *Prog Solid State Chem*, 1989, 19: 47
[28] Heyns A M, Range K J. *J Alloys Compd*, 1991, 176: L17
[29] Courbon H, Formenti M, Pichat P. *J Phys Chem*, 1977, 81: 550
[30] Sato S, Kadowaki T, Yamaguti K. *J Phys Chem*, 1984, 88: 2930

立方Nd_2O_3上过氧物种光诱导生成的^{18}O同位素示踪考察

景孝廉, 余雯瑜, 翁维正*, 李建梅, 夏文生, 万惠霖#
厦门大学化学化工学院化学系, 固体表面物理化学国家重点实验室, 醇醚酯化工清洁生产国家工程实验室, 福建厦门361005

摘要: 采用原位显微Raman光谱和^{18}O同位素示踪技术, 以325 nm激光为激发光源, 对立方Nd_2O_3上过氧物种的光诱导生成过程进行了详细表征, 进一步证实过氧源于分子氧对晶格氧的氧化反应. 结果还表明, 325 nm激光在室温下即可诱导过氧的生成, 在实验条件下, 生成的过氧物种可与Nd_2O_3的晶格氧发生快速的氧交换反应, 位于Nd_2O_3体相的晶格氧也可迁移至样品表层进而参与过氧的生成. 325 nm激光照射有助于促进晶格氧的迁移以及晶格氧与分子氧之间的氧交换反应.

关键词: 分子氧活化; 过氧; 倍半氧化钕; 光诱导反应; ^{18}O同位素研究; Raman光谱

收稿日期: 2014-03-28. 接受日期: 2014-05-14. 出版日期: 2014-08-20.
*通讯联系人. 电话/传真: (0592)2185192; 电子信箱: wzweng@xmu.edu.cn
#通讯联系人. 电话: (0592)2186569; 传真: (0592)2185192; 电子信箱: hlwan@xmu.edu.cn
基金来源: 国家重点基础研究发展计划(973计划, 2010CB732303); 国家自然科学基金(21173173, 21033006, 21373169); 教育部创新团队项目(IRT1036).
本文的英文电子版由Elsevier出版社在ScienceDirect上出版(http://www.sciencedirect.com/science/journal/18722067).

1. 前言

稀土氧化物具有优良的化学和热稳定性以及独特的电子层结构. 对于甲烷氧化偶联和乙烷氧化脱氢等轻质烷烃的临氧催化转化, 稀土氧化物也具有优良的催化性能[1−12]. 探明反应的活性氧物种以及分子氧在稀土氧化物上的活化和转化途径对于深入了解相关反应机理具有重要意义[13−19]. 我们在采用Raman光谱对O_2气氛下的稀土倍半氧化物(Ln_2O_3, Ln = La, Sm, Nd, Gd)进行原位表征时发现, 激光照射可诱导Ln_2O_3表面生成过氧物种[20,21]. 该发现不仅有助于深化对分子氧在阳离子价态不变的金属氧化物表面活化生成活性氧物种机理的认识, 也为分子氧在氧化物表面的活化提供了一条新途径, 因此在光催化选择氧化方面具有潜在应用价值. 在前期工作基础上, 本文采用^{18}O同位素示踪技术对立方Nd_2O_3上过氧物种的光诱导生成过程进行了详细考察, 以期进一步深化对分子氧在阳离子价态不变的金属氧化物表面活化生成活性氧物种机理的认识.

2. 实验部分

2.1. 样品制备

立方Nd_2O_3的制备方法参照文献[22,23]. 将商品Nd_2O_3 (99.99%; Alfa Aesar)在100 °C下用含水蒸气的21% O_2/N_2气流(以鼓泡方式将水蒸气带入)处理100 h, 制得$Nd(OH)_3$. 将$Nd(OH)_3$在干燥的21% O_2/N_2气流中650 °C焙烧3 h制得立方Nd_2O_3样品.

2.2. 常规表征

X射线衍射(XRD)实验在PANalytical公司的X' Pert Pro型X射线粉末衍射仪上进行. 管电流30 mA, 管电压40 kV, 使用X' Celerator超能阵列探测器, 以Cu-K_α (λ = 0.15406 nm)为辐射源, 采用石墨单色器滤光. 扫描区间为10°−90°, 扫描速度为0.0167°/s, 每步时间约24 s.

样品的比表面积(A_{BET} = 6.9 m^2/g)采用BET方法在Micromeritics TriStar II 3020型物理吸附仪上测定. 实验以N_2为吸附质, 吸附温度为–196 °C. 测试前, 样品先在200 °C下抽空处理3 h.

扫描电镜(SEM)实验在Hitachi S-4800型场发射扫描电子显微镜上进行, 加速电压为15 kV. 先将Nd_2O_3样品分散在无水乙醇中, 再将悬浮夜滴在干净的硅片上自然风干后进行SEM表征.

立方Nd_2O_3的XRD和SEM图分别示于图1和图2.

2.3. 原位Raman光谱表征

原位Raman光谱表征实验在配有Leica DMLM显微镜和OFR LMU-15×-NUV物镜以及自行研制的高温原位Raman样品池的Renishaw RT 1000激光显微拉曼光谱仪上进行. 样品池结构见文献[24]. 实验以325 nm激光(He-Cd激光器)为激发光源, 光谱仪的分辨率约为6 cm^{-1}, 聚焦于样品表面的激光光斑直径和最大激光功率分别约为3 μm和3 mW. 摄谱所用激光功率和谱图采集时间依实验不同而不同, 多数实验的激光功率和谱图采集时间分别为0.75 mW和50 s.

合成的立方$Nd_2{}^{16}O_3$样品首先在650 °C下通$^{16}O_2$ (99.995%; Linde; 50 mL/min)处理180−360 min以除去样品上的碳酸盐物种和吸附的水分. 处理后的样品随后在$^{16}O_2$气氛和无光照条件下降至25 °C, 在$^{16}O_2$或$^{18}O_2$气氛下用聚焦后的325 nm激光束连续照射样品并用Raman光谱仪记录样品在光照过程的变化.

^{18}O标记的Nd_2O_3样品由立方$Nd_2{}^{16}O_3$在$^{18}O_2$气流(97%; CIL; 5 mL/min)中于650 °C热处理6 h制得. 处理后的样品随后在$^{18}O_2$气氛和无光照条件下降至25 °C, 在$^{18}O_2$气氛下用聚焦后的325 nm激光束连续照射样品并用Raman光谱仪记录样品在光照过程的变化.

3. 结果与讨论

3.1. $^{16}O_2$和$^{18}O_2$气氛下立方$Nd_2{}^{16}O_3$上过氧物种的光诱导生成

图3(a)为$^{16}O_2$气氛下的立方$Nd_2{}^{16}O_3$在25 ºC下用325 nm激光连续照射过程的Raman谱图的变化. 由图可知, 随激光照射时间增加, 归属于Nd^{3+}–$^{16}O^{2-}$振动的Raman谱带(~331 cm^{-1})强度逐渐减弱, 位于833 cm^{-1}处可归属为$^{16}O_2{}^{2-}$过氧物种O–O键伸缩振动的Raman谱带[20,21,25–27]强度不断增强. 样品经激光连续照射60 min后, 在1300–1800 cm^{-1}范围内还可清晰检出两个位于1554和1646 cm^{-1}的谱峰(图3(b)), 其中位于1646 cm^{-1}的宽峰的波数略低于$^{16}O_2{}^{2-}$过氧物种O–O键伸缩振动频率的2倍, 可归属为过氧物种O–O键伸缩振动的倍频峰. 1554 cm^{-1}谱峰的波数与分子氧($^{16}O_2$)O–O键伸缩振动的波数相近, 但较气相$^{16}O_2$的谱峰(图4)低约2 cm^{-1}, 可指认为吸附于样品表面的分子氧物种, 该物种可能由过氧物种分解所产生. 本文3.2节将提供更多关于该谱峰本质的实验证据.

图5(a)为$^{18}O_2$气氛下立方$Nd_2{}^{16}O_3$在25 °C下用325 nm激光连续照射过程的Raman谱图变化. 可以看出,该谱图的变化规律与图3(a)十分相似. 随照射时间延长,

位于833 cm^{-1}附近的$^{16}O_2^{2-}$谱带逐渐增强，同时Nd^{3+}–$^{16}O^{2-}$ (331 cm^{-1})谱带逐渐减弱. 这清楚地表明$Nd_2{}^{16}O_3$上的晶格氧($^{16}O^{2-}$)物种参与了过氧的生成. 样品经激光连续照射30 min后, 在1300–1800 cm^{-1}范围内可清晰检出三个位于1471, 1554和1640 cm^{-1}的谱峰(图5(b)). 其中位于1640和1554 cm^{-1}的谱峰可分别归属为$^{16}O_2^{2-}$过氧物种的倍频峰和吸附于样品表面的$^{16}O_2$物种的O–O伸缩振动峰; 位于1471 cm^{-1}的谱峰与气相$^{18}O_2$的峰位(图4)一致, 可归属为气相$^{18}O_2$物种的O–O伸缩振动. 鉴于图5的实验是在高纯度$^{18}O_2$ (同位素纯度 > 97%)气流下进行的, 而图5(b)中$^{16}O_2$的谱峰(1554 cm^{-1})强度显著高于气相$^{18}O_2$的谱峰(1471 cm^{-1}), 因此位于1554 cm^{-1}的谱峰不是源于气相的$^{16}O_2$分子, 而是来自样品表面的$^{16}O_2$物种. 由于位于1554 cm^{-1}的表面分子氧谱峰只有在生成了过氧的$Nd_2{}^{16}O_3$样品上才能被清晰检出, 该物种可能源于过氧物种在光照下的分解. 研究表明, 488 nm激光的照射可导致$NdO_2(O_2)$ (Nd的过氧化合物)的分解[28].

前期研究表明, 分子氧的存在是稀土倍半氧化物上过氧生成的必要条件之一, 过氧物种由光照下分子氧对稀土倍半氧化物的晶格氧的氧化反应所产生[20,21]. 这表明在以$^{18}O_2$和$^{16}O^{2-}$为反应物的情况下, 所生成的产物中将含有^{18}O标记过氧物种. 然而图5只检测到与$^{16}O_2^{2-}$ (833 cm^{-1})对应的过氧物种. 这可能是由于生成的过氧物种与$Nd_2{}^{16}O_3$的晶格氧之间发生了快速的氧交换反应. 由于$^{16}O^{2-}$是Nd_2O_3表面丰度最大的氧物种, ^{18}O标记的过氧物种与$Nd_2{}^{16}O_3$的晶格氧之间的快速氧交换最终将导致$^{16}O_2^{2-}$的生成. 由于晶格氧与表面过氧或分子氧之间的快速氧交换, 由过氧分解产生的表面分子氧物种(1554 cm^{-1})所含的氧同位素与过氧物种中的氧同位素完全相同. 可见, 在以^{18}O为示踪原子的实验中, 我们可借助样品上吸附态分子氧的同位素谱峰来判断Nd_2O_3表面是否生成了同位素标记的过氧物种. 与过氧物种的Raman峰相比, 表面吸附态分子氧Raman峰的峰宽要窄得多, 因此具有更高的分辨率.

3.2. $^{18}O_2$气氛下^{18}O标记的立方Nd_2O_3上过氧物种的光诱导生成

为了探明Nd_2O_3上过氧物种的光诱导生成机理, 我们进一步在$^{18}O_2$气氛下对^{18}O标记的立方Nd_2O_3样品的过氧物种光诱导生成进行了考察. 实验所用^{18}O标记的Nd_2O_3样品系通过将$Nd_2{}^{16}O_3$在650 °C和$^{18}O_2$气氛下处理6 h并在$^{18}O_2$气氛下降至25 °C获得. 与$Nd_2{}^{16}O_3$样品的Raman谱相比, 处理后的样品上氧化钕的Nd^{3+}–O^{2-}特征振动峰由336 cm^{-1}红移至320 cm^{-1}. 后者与采用谐振子模型(假设Nd^{3+}–$^{16}O^{2-}$的振动频率为336 cm^{-1})计算出的Nd^{3+}–$^{18}O^{2-}$键的振动波数(319 cm^{-1})十分接近, 表明在Raman光谱的检测深度内^{18}O标记的立方Nd_2O_3样品表面绝大多数的晶格氧物种已被$^{18}O^{2-}$所取代. 图6(a)为^{18}O标记的立方Nd_2O_3在25 °C和$^{18}O_2$气氛下用325 nm激光连续照射过程的Raman谱图变化情况. 在照射了1 min的样品上可清晰检出位于789 cm^{-1}的Raman谱带, 随照射时间增加, 在811 cm^{-1}处还出现一个肩峰, 该峰在激光照射15 min后已非常明显. 在经325 nm激光照射30 min后样品上可清晰检出三个位于1468, 1510和1554 cm^{-1}的Raman峰(图6(b)). 采用谐振子模型并以$^{16}O_2^{2-}$过氧的伸缩振动频率(833 cm^{-1})为基准, 可计算出$^{18}O_2^{2-}$和$(^{18}O^{16}O)^{2-}$等过氧物种氧–氧键的伸缩振动波数分别为789和810 cm^{-1}. 同理, 以位于1556 cm^{-1}的$^{16}O_2$分子氧伸缩振动频率为基准, 可计算出$^{18}O_2$和$^{18}O^{16}O$等分子氧物种的氧–氧键伸缩振动波数分别1467和1512 cm^{-1}. 可以看出, 计算所得的^{18}O标记过氧和分子氧物种的振动频率与图6结果十分吻合, 由于实验是在同位素纯度优于97%的$^{18}O_2$气流中进行的, 图6(b)中位于1510和1554 cm^{-1}处的谱峰只能分别来自^{18}O标记的Nd_2O_3样品表面的$^{18}O^{16}O$和$^{16}O_2$等分子氧物种. 鉴于图6(b)中$^{18}O_2$和$^{16}O_2$谱峰的强度比显著高于图5(b)中相同物种的强度比, 且与图4中气相$^{18}O_2$的Raman峰相比, 图6(b)中$^{18}O_2$的峰位向低频方向位移了约3 cm^{-1}, 可合理地认为, 图6(b)中位于1468 cm^{-1}的谱峰主要也来自样品表面的$^{18}O_2$物种. 这些结果表明, 在图6的实验条件下, ^{18}O标记的Nd_2O_3样品表面生成了$^{18}O_2^{2-}$, $(^{18}O^{16}O)^{2-}$和$^{16}O_2^{2-}$等过氧物种. 由于实验是在$^{18}O_2$气流中进行的, $(^{18}O^{16}O)^{2-}$和$^{16}O_2^{2-}$等过氧物种中的^{16}O原子只能来源于^{18}O标记的Nd_2O_3样品, 这进一步证实Nd_2O_3上的晶格氧物种参与了过氧的生成. 结果还表明, 虽然经历了650 °C通$^{18}O_2$气流处理6 h, $Nd_2{}^{16}O_3$样品上的^{16}O并未被^{18}O完全取代.

从图6(a)中Raman谱图的变化趋势可以看出, 由于^{18}O标记的Nd_2O_3样品表面的绝大多数晶格氧物种已被$^{18}O^{2-}$取代, 分子氧($^{18}O_2$)首先与样品表面的$^{18}O^{2-}$反应生成$^{18}O_2^{2-}$过氧物种(789 cm^{-1}). 随着激光照射时间的延长, 样品表面还检测到与$(^{18}O^{16}O)^{2-}$ (811 cm^{-1})对应的过氧谱峰以及与$^{18}O^{16}O$ (1510 cm^{-1})和$^{16}O_2$ (1554 cm^{-1})对应的表面分子氧谱峰(图6(b)). 图6(a)中的$(^{18}O^{16}O)^{2-}$过氧物种可由氧化钕体相的$^{16}O^{2-}$迁移到样品表面再与$^{18}O_2$反应直接生成, 也可通过迁移到样品表面的$^{16}O^{2-}$与$^{18}O_2^{2-}$之间的

同位素交换反应生成. 生成的($^{18}O^{16}O)^{2-}$也可进一步通过与$^{16}O^{2-}$的同位素交换反应转化为$^{16}O_2^{2-}$过氧物种, 后者在实验条件下可分解生成吸附于样品表面的$^{16}O_2$分子氧物种(1554 cm^{-1}). 325 nm激光的照射对$^{16}O^{2-}$的迁移及其与$^{18}O_2^{2-}$的交换可能具有促进作用, 为了获得相关的实验证据, 我们进一步在25 °C和$^{18}O_2$气氛下考察了激光功率(0.3和3 mW)对^{18}O标记的Nd_2O_3上过氧物种光诱导生成的影响. 如图7所示, 在用0.3 mW激光照射的14 min过程中, 样品上仅检测到位于790 cm^{-1}的$^{18}O_2^{2-}$过氧物种(图7(a)), 说明在实验条件下几乎不发生$^{16}O^{2-}$的迁移以及$^{16}O^{2-}$与$^{18}O_2^{2-}$之间的同位素交换反应. 当激光功率提高到3 mW后, 过氧谱带的峰宽显著增大(图7(b)), 在照射了5–20 min的样品上可清晰检出$^{18}O_2^{2-}$ (790 cm^{-1})和($^{18}O^{16}O)^{2-}$ (811 cm^{-1})的过氧谱带, 说明激光照射的确对晶格氧迁移及其与过氧之间的氧同位素交换反应具有促进作用. 研究表明, 光照可诱导$^{18}O_2$与TiO_2晶格氧之间的同位素交换[29,30].

4. 结论

分子氧可通过在光的诱导下与立方Nd_2O_3的晶格氧反应转化为过氧物种, 在325 nm激光的照射下, 上述反应在室温下即可发生. 以^{18}O为示踪原子的实验表明, 生成的过氧物种可与Nd_2O_3的晶格氧发生快速的氧交换反应, 位于Nd_2O_3体相的晶格氧也可迁移至样品表层进而参与过氧的生成. 325 nm激光的照射有助于促进晶格氧的迁移以及晶格氧与分子氧之间的氧交换.